On the Apparently Anomalous Distance Dependence of Charge-Transfer Rates in 9-Amino-6-chloro-2-methoxyacridine-Modified DNA

Stephan Hess, Mirco Götz, William B. Davis,*,† and Maria-Elisabeth Michel-Beyerle*

Contribution from the Institut für Physikalische und Theoretische Chemie, Technische Universität München, Lichtenbergstrasse 4, 85748 Garching, Germany

Received April 16, 2001

Abstract: From previous thermal and photoinduced charge-transfer reactions in duplex DNA there is accumulative evidence for an attenuation parameter β of the distance dependence in the range 0.6−0.8 Å^{-1}, with the exception of one specific system exhibiting $\beta = 1.5$ Å^{-1} which is reinvestigated in this paper. Femtosecond to nanosecond time-resolved pump−probe spectroscopy has been used to follow photoinduced charge-shift dynamics in DNA duplexes containing a covalently appended, protonated 9-alkylamino-6-chloro-2-methoxyacridine chromophore. This acridine derivative (X^+) resides in the DNA duplex at a specific abasic site, which is highly defined as reflected in the monoexponentiality of the kinetics. In the presence of only neighboring A:T base pairs, no charge transfer occurs within the excited-state lifetime (18 ns) of the chromophore. However, the presence of a guanine nucleobase as either a nearest neighbor or with one interspersed A:T base pair does result in fluorescence quenching. In the case of nearest neighbors, the intermediate radical state $X^\bullet$ is formed within 4 ps and decays on the 30 ps time scale. Placing one A:T base pair between the X^+ and guanine slows down the forward transfer rate by 3 orders of magnitude, corresponding to an apparent β value of >2.0 Å^{-1}. This dramatic decrease in the rate is due to a change in charge-transfer mechanism from a (nearly) activationless to a thermally activated regime in which the forward transfer is slower than the back transfer and the $X^\bullet$ state is no longer observed. These observations indicate that the distance dependence of charge injection in the X^+-labeled DNA duplex is not solely caused by a decrease in electronic couplings but also by a concomitant increase of the activation energy with increasing distance. This increase in activation energy may result from the loss of driving force due to excited-state relaxation competing with charge transfer, or reflect distance-dependent changes in the energetics, predominantly of the low-frequency reorganization energy in this charge-shift reaction, on purely electrostatic grounds. To test the hypothesis of distance-dependent activation energy, guanine has been replaced by 7-deazaguanine, its easier-to-oxidize purine analogue. In these duplexes, a similar change of charge-transfer mechanism is found. However, consistent with an a priori larger driving force this change occurs at a larger donor−acceptor separation than in the X^+-guanine systems. Independent of the detailed contributions to the distance-dependent activation energy, this phenomenon illustrates the complex nature of experimental β values.

1. Introduction

Charge migration phenomena in DNA are the subject of intense current research.[1−6] The worldwide activities are driven to a large extent by the implication of electronic conduction in both the pathways of oxidative damage[7] and the development of electrochemical biosensoric[8−10] and nanoelectronic devices.[11−13] In the early 1990s, vivid interest in this field was stimulated by the provocative twin conjectures of DNA being a "molecular wire" which gives rise to "chemistry at a distance".[14−17] In fact, the molecular wire concept is reminiscent of aromatic hydrocarbon crystals[18] in which the two extreme modes of carrier transport can exist: excess carriers may be delocalized, exhibiting a relatively large mean free path or they may be localized for example in a potential well caused by a polarization of the lattice, and consequently move in a thermally activated hopping process. Independent of the type of carrier motion, chemical

* To whom correspondence should be addressed.
† Present address: School of Molecular Biosciences, Washington State University, Pullman, Washington 99164-4660.

(1) Giese, B. *Acc. Chem. Res.* **2000**, *33*, 631−636.
(2) Lewis, F. D.; Letsinger, R. L.; Wasielewski, M. R. *Acc. Chem. Res.* **2001**, *34*, 159−170.
(3) Schuster, G. B. *Acc. Chem. Res.* **2000**, *33*, 253−260.
(4) Diederichsen, U. *Angew. Chem., Int. Ed. Engl.* **1997**, *36*, 2317−2319.
(5) Ratner, M. A. *Nature* **1999**, *397*, 480−481.
(6) Grinstaff, M. W. *Angew. Chem., Int. Ed.* **1999**, *38*, 3629−3635.
(7) Burrows, C. J.; Muller, J. G. *Chem. Rev.* **1998**, *98*, 1109−1152.
(8) Hartwich, G.; Caruana, C. J.; de Lumley-Woodyear, T.; Wu, Y.; Campbell, C. N.; Heller, A. *J. Am. Chem. Soc.* **1999**, *121*, 10803−10812.
(9) Lisdat, F.; Ge, B.; Scheller, F. W. *Electrochem. Commun.* **1999**, *1*, 65−67.
(10) Boon, E. M.; Ceres, D. M.; Drummond, T. G.; Hill, M. G.; Barton, J. K. *Nature Biotechnol.* **2000**, *18*, 1096−1100.
(11) Braun, E.; Eichen, Y.; Sivan, U.; Ben-Joseph, G. *Nature* **1998**, *391*, 775−778.
(12) Fink, H.-W.; Schönenberger, C. *Nature* **1999**, *398*, 407−410.
(13) Porath, D.; Bezryadin, A.; De Vries, S.; Dekker: C. *Nature* **2000**, *403*, 635−638.
(14) Murphy, C. J.; Arkin, M. R.; Jenkins, Y.; Ghatlia, N. D.; Bossmann, S. H.; Turro, N. J.; Barton, J. K. *Science* **1993**, *262*, 1025−1029.
(15) Murphy, C. J.; Arkin, M. R.; Ghatlia, N. D.; Bossmann, S. H.; Turro, N. J.; Barton, J. K. *Proc. Natl. Acad. Sci. U.S.A.* **1994**, *91*, 5315−5319.
(16) Arkin, M. R.; Stemp, E. D. A.; Holmlin, R. E.; Barton, J. K.; Hörmann, A.; Olson, E. J. C.; Barbara, P. F. *Science* **1996**, *273*, 475−479.
(17) Turro, N. J.; Barton, J. K. *J. Biol. Inorg. Chem.* **1998**, *3*, 201−209.
(18) Pope, M.; Swenberg, C. E. *Electronic Processes in Organic Crystals*; Clarendon Press: Oxford, 1982.

10.1021/ja010976r CCC: $20.00
Published on Web 09/22/2001

side reactions of charge carriers can occur at surface sites which correspond to the macroscopic dimensions of the crystal.

As applied to DNA, the notion of "chemistry at a distance" rests upon reactive intermediates, for example, oxidized guanines, which migrate from the site of generation to a distant site of reaction. In this case of transport of positive charges (holes), analyses of DNA strand cleavage patterns have shown that distances of about 200 Å can be spanned in a (almost) distance-independent fashion.[19] In contrast to an aromatic crystal, the description of long-range hole transport in the duplex is complicated by the different energetics of the nucleobases, that is, the different oxidation potentials of guanine (G), adenine (A), thymine (T) and cytosine (C).[20] Experiments and theory led to the conclusion that in a duplex constructed of G:C base pairs separated by short A:T sequences (up to four base pairs),[21,22] holes propagate by hopping between the nucleobases with the lowest oxidation potential, that is, the guanines. Depending on the number of steps, the hopping mechanism for long-range hole transport is characterized by either a weak algebraic or weak exponential distance dependence.[23,24] During the individual hopping steps between any two guanines the A:T base pairs do not form kinetic intermediates. Instead they increase the electronic coupling between the guanines through the superexchange interaction. This behavior reflects the hierarchy of the in vitro oxidation potentials of the nucleobases in aqueous and nonaqueous solution where the oxidation potential of adenine is by about 0.4 eV higher than that of guanine.[20,25] Thus, for the single-step hole transfer three out of four nucleobases, that is, A, and to a lesser extent T and C, act as superexchange mediators while one of them, G, plays the role of a charge-relay station. Finally, the recent attempts to successfully explain long-range hole transport between guanines separated by a large number of A:T base pairs should be mentioned.[1,3,19] Depending on both the lifetime of the guanine cation and the energy separation given by the in situ oxidation potentials of guanine and adenine, a switch of mechanism is observed[21] and theoretically modeled.[22] Upon the breakdown of single-step superexchange couplings in the presence of more than four A:T base pairs, thermally activated oxidation of adenines and hole transport along a nearest-neighbor A:T sequence may take over. Thermal population of the A:T bridge states and long-range charge transport across a delocalized bridge system are also the basic features of an early attempt to describe long-range charge transport in duplex DNA.[26]

This simplified picture is the cumulative result of the considerable experimental[1−3,17,27−32] and theoretical[23,24,26,33−42] efforts which followed the observations of long-range charge transport phenomena in duplex DNA. Since it was possible to describe the extensive sets of hole-transport experiments performed by Giese and co-workers[1,21,43−45] in a self-consistent way within the frame of the "simple" hopping model,[33,34] it seems that on a rudimentary level the problem of long-range hole transport in DNA has been solved. The present discussion appears to be converging toward a weakly distance-dependent hopping mechanism which is also the bottom line of a more complex "phonon-assisted polaron-like" hopping mechanism.[3,46]

This stage of qualitative understanding has not quite been reached for the subject of this paper, the distance dependence of the injection process. In any simple donor−bridge−acceptor system the dependence of an electron-transfer rate on the donor−acceptor distance R is described by the Marcus−Levich−Jortner equation[47−51]

$$k_{ET} = \frac{2\pi}{\hbar} V_0^2 \exp(-\beta R)\mathrm{FC} \qquad (1)$$

The term $V_0 \exp[-(\beta/2)R]$ is (approximately) the electronic coupling V for the transfer process, and it is characterized by the electronic coupling at donor−acceptor closest contact, V_0, and an attenuation parameter, β, which depends on the electronic coupling of both donor and acceptor to the bridge and the vertical energy gap between the donor and the bridge states. The FC term comprises the thermally averaged nuclear Franck−Condon density of states involving high-frequency intramolecular vibrations and a nuclear reorganization energy λ_i, the low-frequency reorganization energy λ_s, which is (mostly) related to the response of the medium to changes in the charge distribution, as well as the change in Gibbs free energy ΔG driving the electron-transfer reaction. The FC factor in its quantum mechanical formulation (eq 1) is of special importance for highly exoergic reactions since it provides for the explanation of experimental electron-transfer rates which are larger than the

(19) Núñez, M. E.; Hall, D. B.; Barton, J. K. *Chem. Biol.* **1999**, *6*, 85−97.
(20) Seidel, C. A. M.; Schulz, A.; Sauer, M. H. M. *J. Phys. Chem.* **1996**, *100*, 5541−5553.
(21) Giese, B.; Spichty, M. *ChemPhysChem* **2000**, *1*, 195−198.
(22) Bixon, M.; Jortner, J. *J. Am. Chem. Soc.* Submitted.
(23) Jortner, J.; Bixon, M.; Langenbacher, T.; Michel-Beyerle, M. E. *Proc. Natl. Acad. Sci. U.S.A.* **1998**, *95*, 12759−12765.
(24) Berlin, Y. A.; Burin, A. L.; Ratner, M. A. *J. Phys. Chem. A* **2000**, *104*, 443−445.
(25) Steenken, S.; Jovanovic, S. V. *J. Am. Chem. Soc.* **1997**, *119*, 617−618.
(26) Felts, A. K.; Pollard, W. T.; Friesner, R. A. *J. Phys. Chem.* **1995**, *99*, 2929−2940.
(27) Wan, C.; Fiebig, T.; Schiemann, O.; Barton, J. K.; Zewail, A. H. *Proc. Natl. Acad. Sci. U.S.A.* **2000**, *97*, 14052−14055.
(28) Harriman, A. *Angew. Chem., Int. Ed.* **1999**, *38*, 945−949.
(29) Shafirovich, V.; Dourandin, A.; Huang, W.; Luneva, N. P.; Geacintov, N. E. *Phys. Chem. Chem. Phys.* **2000**, *2*, 4399−4408.
(30) Yoshioka, Y.; Kitagawa, Y.; Takano, Y.; Yamaguchi, K.; Nakamura, T.; Saito, I. *J. Am. Chem. Soc.* **1999**, *121*, 8712−8719.
(31) Nakatani, K.; Dohno, C.; Saito, I. *J. Am. Chem. Soc.* **2000**, *122*, 5893−5894.
(32) Fukui, K.; Tanaka, K.; Fujitsuka, M.; Watanabe, A.; Ito, O. *J. Photochem. Photobiol., B* **1999**, *50*, 18−27.
(33) Bixon, M.; Giese, B.; Wessely, S.; Langenbacher, T.; Michel-Beyerle, M. E.; Jortner, J. *Proc. Natl. Acad. Sci. U.S.A.* **1999**, *96*, 11713−11716.
(34) Bixon, M.; Jortner, J. *J. Phys. Chem. B* **2000**, *104*, 3906−3913.
(35) Voityuk, A. A.; Jortner, J.; Bixon, M.; Rösch, N. *Chem. Phys. Lett.* **2000**, *324*, 430−434.
(36) Voityuk, A. A.; Rösch, N.; Bixon, M.; Jortner, J. *J. Phys. Chem. B* **2000**, *104*, 9740−9745.
(37) Voityuk, A. A.; Jortner, J.; Bixon, M.; Rösch, N. *J. Chem. Phys.* **2001**, *114*, 5614−5620.
(38) Grozema, F. C.; Berlin, Y. A.; Siebbeles, L. D. A. *J. Am. Chem. Soc.* **2000**, *122*, 10903−10909.
(39) Berlin, Y. A.; Burin, A. L.; Ratner, M. A. *J. Am. Chem. Soc.* **2001**, *123*, 260−268.
(40) Pollard, W. T.; Felts, A. K.; Friesner, R. A. *Adv. Chem. Phys.* **1996**, *93*, 77−134.
(41) Priyadarshy, S.; Risser, S. M.; Beratan, D. N. *J. Phys. Chem.* **1996**, *100*, 17678−17682.
(42) Okada, A.; Chernyak, V.; Mukamel, S. *J. Phys. Chem. A* **1998**, *102*, 1241−1251.
(43) Giese, B.; Wessely, S.; Spormann, M.; Lindemann, U.; Meggers, E.; Michel-Beyerle, M. E. *Angew. Chem., Int. Ed.* **1999**, *38*, 996−998.
(44) Meggers, E.; Michel-Beyerle, M. E.; Giese, B. *J. Am. Chem. Soc.* **1998**, *120*, 12950−12955.
(45) Meggers, E.; Kusch, D.; Spichty, M.; Wille, U.; Giese, B. *Angew. Chem., Int. Ed.* **1998**, *37*, 460−462.
(46) Henderson, P. T.; Jones, D.; Hampikian, G.; Kan, Y.; Schuster, G. B. *Proc. Natl. Acad. Sci. U.S.A.* **1999**, *96*, 8353−8358.
(47) Levich, V. O. *Adv. Electrochem.* **1966**, *4*, 249−371.
(48) Kestner, N. R.; Logan, J.; Jortner, J. *J. Phys. Chem.* **1974**, *78*, 2148−2166.
(49) Ulstrup, J.; Jortner, J. *J. Chem. Phys.* **1975**, *63*, 4358−4368.
(50) Jortner, J. *J. Chem. Phys.* **1976**, *64*, 4860−4867.
(51) Marcus, R. A. *J. Chem. Phys.* **1984**, *81*, 4494−4500.

ones given by the classical Marcus expression:[52,53]

$$FC = (4\pi\lambda_s k_B T)^{-(1/2)} \exp\left(\frac{-(\Delta G + \lambda_s)^2}{4\lambda_s k_B T}\right) \qquad (2)$$

where k_B denotes the Boltzmann constant and T the temperature. Throughout this paper, the qualitative arguments concerning activated or activationsless reactions will be based on this simple formalism.

The value of the parameter β in eq 1 for the transfer of holes has been one of the most contentious points in the DNA charge-transfer literature. The Barton group's earliest estimates of β came from experiments utilizing DNA duplexes with hole injectors and acceptors tethered to the 5′ termini with relatively long linkers, allowing for multiple intercalation sites.[14] In the absence of any monitoring of the charge-transfer intermediates in their experiments, they concluded that DNA must have a small β, that is, $\beta < 0.2$ Å^{-1}. In other experiments, Brun and Harriman[54] also extracted β from noncovalently attached, intercalated donors and acceptors and obtained a value in the range of 0.9 Å^{-1}. While the β values reported from these two different experiments are in sharp disagreement, a reconciliation between them is not possible due to poor structural definition of these charge-transfer systems. A more precise definition of the donor−acceptor distance has become possible in oligonucleotides where the hole injector is either a specific ribose cation,[44] a covalently attached hole-injecting chromophore,[32,55] or a nucleobase analogue[27,29] which is capable of acting as a hole-donating species. These newer assays have allowed studies on the dependence of both thermal and photoinduced hole-transfer processes on the number of A:T pairs separating the donor and acceptor species. In the thermal hole-transfer studies of Giese and co-workers,[44] hole transfer from a guanine cation, selectively oxidized by a ribose cation, to a triple guanine (GGG) led to distance-dependent yields of strand-cleavage products. A second thermal hole-transfer system comes from Geacintov and co-workers,[29] where two photon ionization of the nucleobase analogue 2-aminopurine produces a 2-aminopurine radical cation ($2aP^{\bullet+}$), and the distance dependence of hole transfer from $2aP^{\bullet+}$ to a neighboring G was monitored via the transient absorption of $G^{\bullet+}$. Photoinduced hole-transfer reactions have been studied in chromophore-labeled duplexes using femtosecond to microsecond time-resolved pump−probe spectroscopy or fluorescence lifetime measurements. The oxidation dynamics of guanine are deduced from either the excited-state behavior of the hole-injecting chromophore, as in systems containing a protonated 9-alkylamino-6-chloro-2-methoxyacridine, X^+, (Chart 1) intercalated at an abasic site[32] or an excited nucleobase analogue within the duplex, that is, 2-aminopurine,[27] or by observation of the charge-transfer intermediate state as in the capped stilbene hairpins.[55,56]

Despite the different nature of these experiments, both the yield of strand-cleavage products as well as the directly measured hole-injection rate k_{HT} decrease exponentially with the number of A:T base pairs between the hole donor and guanine. As for the value of β, both thermal and photoinduced hole-transfer processes have yielded $\beta \approx 0.6-0.8$ Å^{-1}. This β range is larger than that observed for donor−acceptor systems connected by π-conjugated bridges[57−61] and significantly smaller than that for nonspecific electron-transfer pathways in proteins[62−65] and rigid aliphatic bridges[66−69] which range between 1 and 1.4 Å^{-1}. The only exception to this range of β values in DNA arises in the experiments involving X^+-labeled DNA duplexes, where the decrease of k_{HT} with increasing distance is much steeper and $\beta = 1.5$ Å^{-1}.[32] On the theory front, β values in the range $\sim$0.6−0.8 Å^{-1} were substantiated by recent quantum chemical calculations.[36,37]

Chart 1. Chemical Structure of the X^+ Modification Utilized in This Work, along with the Structures of Guanine (G) and 7-Deazaguanine (Z)

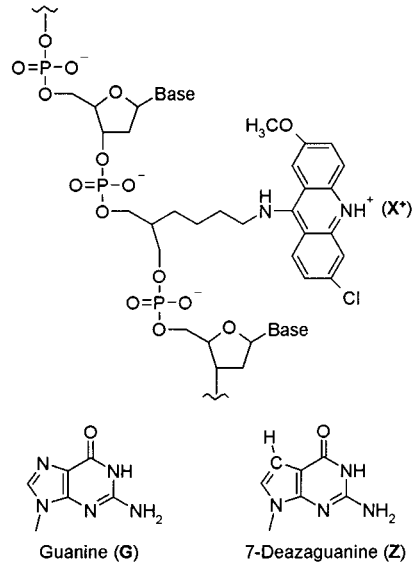

The large β value reported for X^+/DNA may be system-inherent, and differences in attenuation factors could originate from specific electronic couplings between the different charge-injecting species and one or more bridging A:T pairs. Moreover, the electronic couplings may be affected by large-amplitude motions of this modified duplex and therefore may be time-dependent. In addition, some of the energy parameters which govern the hole-transfer rate, such as ΔG and λ_s, may have a distance dependence of their own.[52,70] This last hypothesis

(52) Marcus, R. A. *J. Chem. Phys.* **1956**, *24*, 966−978.
(53) Marcus, R. A.; Sutin, N. *Biochim. Biophys. Acta* **1985**, *811*, 265−322.
(54) Brun, A. M.; Harriman, A. *J. Am. Chem. Soc.* **1992**, *114*, 3656−3660.
(55) Lewis, F. D.; Wu, T.; Zhang, Y.; Letsinger, R. L.; Greenfield, S. R.; Wasielewski, M. R. *Science* **1997**, *277*, 673−676.
(56) Lewis, F. D.; Wu, T.; Liu, X.; Letsinger, R. L.; Greenfield, S. R.; Miller, S. E.; Wasielewski, M. R. *J. Am. Chem. Soc.* **2000**, *122*, 2889−2902.
(57) Sachs, S. B.; Dudek, S. P.; Hsung, R. P.; Sita, L. R.; Smalley, J. F.; Newton, M. D.; Feldberg, S. W.; Chidsey, C. E. D. *J. Am. Chem. Soc.* **1997**, *119*, 10563−10564.
(58) Creager, S.; Yu, C. J.; Bamdad, C.; O'Connor, S.; MacLean, T.; Lam, E.; Chong, Y.; Olsen, G. T.; Luo, J.; Gozin, M.; Kayyem, J. F. *J. Am. Chem. Soc.* **1999**, *121*, 1059−1064.
(59) Davis, W. B.; Svec, W. A.; Ratner, M. A.; Wasielewski, M. R. *Nature* **1998**, *396*, 60−63.
(60) Finckh, P.; Heitele, H.; Volk, M.; Michel-Beyerle, M. E. *J. Phys. Chem.* **1988**, *92*, 6584−6590.
(61) Benniston, A. C.; Goulle, V.; Harriman, A.; Lehn, J.-M.; Marczinke, B. *J. Phys. Chem.* **1994**, *98*, 7798−7804.
(62) Page, C. C.; Moser, C. C.; Chen, X.; Dutton, P. L. *Nature* **1999**, *402*, 47−51.
(63) Mutz, M. W.; Case, M. A.; Wishart, J. F.; Ghadiri, M. R.; McLendon, G. L. *J. Am. Chem. Soc.* **1999**, *121*, 858−859.
(64) Isied, S. S.; Ogawa, M. Y.; Wishart, J. F. *Chem. Rev.* **1992**, *92*, 381−394.
(65) Winkler, J. R.; Gray, H. B. *Chem. Rev.* **1992**, *92*, 369−397.
(66) Closs, G. L.; Miller, J. R. *Science* **1988**, *240*.
(67) Leland, B. E.; Joran, A. D.; Felker, P. M.; Hopfield, J. J.; Zewail, A. H.; Dervan, P. B. *J. Am. Chem. Soc.* **1985**, *89*, 5571−5573.
(68) Oevering, H.; Paddon-Row, M. N.; Heppener, M.; Oliver, A. M.; Cotsaris, E.; Verhoeven, J. W.; Hush, N. S. *J. Am. Chem. Soc.* **1987**, *109*, 3258−3269.
(69) Carter, M. J.; Rowe, G. K.; Richardson, J. N.; Tender, L. M.; Terrill, R. H.; Murray, R. W. *J. Am. Chem. Soc.* **1995**, *117*, 2896−2899.

addresses an inherent problem of electron-transfer theory which, in relation to DNA, has been approached recently in an explicit way.[71]

Before invoking these more intricate charge-transfer mechanisms as the origin of the reported steep distance dependence in the X^+/DNA duplexes, it seems useful to study these donor/acceptor systems in fuller detail. In the previous work of Tanaka and co-workers, the X^+ chromophore was covalently attached to the sugar−phosphate backbone using a proprioamide linker and resided inside the duplex by filling an abasic pocket.[32,72−75] Only the dependence of the X^+ fluorescence quenching rate upon the distance between X^+ and G was used to measure β in these duplexes. The identity and fate of any intermediate charge-transfer states were not monitored in these experiments; therefore, no information was obtained about processes which can either compete with or complicate these transfer reactions. One excited-state process which cannot compete with charge transfer at near neutral pH values is deprotonation, because the pK_a value of X^+ does not change upon photoexcitation.[76,77] As an aside, we note that, in its excited state, electron transfer from guanine to $^1(X^+)^*$ should occur via a charge-shift reaction instead of a charge-separation reaction when neutral injectors[2,3] are used. Due to this feature X^+ should be, in principle, an ideal candidate to initiate long-range hopping motion since the Coulombic barrier in a charge-shift reaction should be minimal, thus allowing hopping to favorably compete with electron back transfer.

While X^+ appears to be a perfect hole-injecting chromophore in DNA charge-transfer studies, it must be kept in mind that the X^+ analogue with a primary 9-amino group free in aqueous solution displays complicated photophysics.[77,78] Using steady-state and nanosecond time-resolved fluorescence measurements Hélène and co-workers[77] report a pronounced wavelength dependence of the fluorescence decay, that is, a dynamic Stokes shift, which has been assigned to an environmentally sensitive excited-state relaxation. The relaxation time scale was solvent- and temperature-dependent, ranging from ∼100 ps in glycerol at 10 °C up to 2.5 ns in aqueous solution at room temperature. The relaxation mechanism was ascribed to the response of the polar solvent cage to an inferred 13 D increase of the molecule's dipole moment upon excitation.[77] Since in this work excited-state relaxation has been claimed to depend in a specific way on the microenvironment of the chromophore, intercalation of X^+ in the DNA duplex may influence the time scale of this relaxation process. In this context it is interesting to add that the dynamic Stokes shift of a coumarin dye incorporated into an oligonucleotide in place of a normal purine−pyrimidine base pair occurs with components near 300 ps and 13 ns as measured with a 100 ps time resolution.[79] The total Stokes shift in this system has been expected to be roughly 1500 cm^{-1}. Thus, in view of a possible excited-state relaxation in $^1(X^+)^*$, the steep distance dependence reported for the X^+/DNA system could be caused by the superposition of two effects: a decrease of both the superexchange electronic coupling and the driving force ΔG of the electron-transfer process.

Chart 2. Base Sequences of the X^+-Modified Single Strands[a]

Duplex	1	2	3
X^+(AT)	A	A	A
5'-X^+G	G	A	A
5'-X^+AG	A	G	A
5'-X^+AAG	A	A	G
5'-X^+Z	Z	A	A
5'-X^+AZ	A	Z	A
5'-X^+AAZ	A	A	Z
3'-X^+G	A	A	G
3'-X^+AG	A	G	A
3'-X^+AAG	G	A	A
3'-X^+Z	A	A	Z
3'-X^+AZ	A	Z	A
3'-X^+AAZ	Z	A	A

Duplexes X^+(AT) and 5'-X^+

5'-GCG TTA TAT A(**X^+**)**1 23**T TAT GCG-3'

Duplexes 3'-X^+

5'-GCG TTA **T12 3**(**X^+**)A TAA TAT GCG-3'

[a] The counterstrands used to produce the duplexes are not shown; however, all nucleobases were placed in a standard Watson−Crick pair, and an adenine was placed opposite X^+, similar to the previous work of Tanaka and coworkers.[74]

In the following we present time-resolved spectroscopic studies on a family of X^+-labeled DNA duplexes (Chart 2) where photoexcited X^+ acts as a hole injector and guanine is the hole acceptor. By monitoring three observables, the decay of $^1(X^+)^*$, the formation of the $X^\bullet$ hole-transfer intermediate, and the recovery of the ground state of X^+ in femtosecond transient absorption experiments, we investigate the hole-transfer rates as well as the underlying mechanism, as the distance between X^+ and G is varied in these duplexes. In addition, we make use of an approach to (at least partially) compensate for the potential loss of driving force, induced by X^+ excited-state relaxation, by replacing the electron-donor guanine with its easier to oxidize analogue 7-deazaguanine[22,80] (Z) (Chart 1).

2. Experimental Results

2.1. Steady-State Absorption and Fluorescence. All spectra were measured at 283 K using the procedures outlined in the Experimental section. The absorption and fluorescence spectra of duplex X^+(AT) shown in Figure 1a are representative examples for all duplexes studied. The absorption spectrum is typical for an intercalated 9-amino-6-chloro-2-methoxyacridine chromophore, with $S_0 \rightarrow S_1$ absorption vibronic bands at 452, 428, and 405 nm, and $S_0 \rightarrow S_2$ vibronic bands at 344 and 328 nm.[81]

The fluorescence spectrum of X^+ in all duplexes was obtained using excitation at 390 nm, and the spectrum for X^+(AT) is shown in Figure 1a as an example. The fluorescence spectrum of X^+ in all duplexes shows a main peak at 499 nm, and two sidebands at 471 and 530 nm. These sidebands are indicative of X^+ intercalation into the DNA base stack.[74] The steady-state fluorescence yield from X^+ was found to be highly dependent upon the nucleobase sequence flanking this chromophore (Figure 1b). In samples containing Z a lower fluorescence intensity (vide

(70) Liu, Y.-P.; Newton, M. D. *J. Phys. Chem.* **1994**, *98*, 7162−7169.
(71) Tavernier, H. L.; Fayer, M. D. *J. Phys. Chem. B* **2000**, *104*, 11541−11550.
(72) Fukui, K.; Tanaka, K. *Nucleic Acids Res.* **1996**, *24*, 3962−3967.
(73) Fukui, K.; Iwane, K.; Shimidzu, T.; Takano, Y. *Tetrahedron Lett.* **1996**, *37*, 4983−4986.
(74) Fukui, K.; Tanaka, K. *Angew. Chem., Int. Ed.* **1998**, *37*, 158−161.
(75) Fukui, K.; Morimoto, M.; Segawa, H.; Tanaka, K.; Shimidzu, T. *Bioconjugate Chem.* **1996**, *7*, 349−355.
(76) Capomacchia, A. C.; Schulman, S. G. *Anal. Chim. Acta* **1975**, *77*, 79−85.
(77) Sun, J.; Rougée, M.; Delarue, M.; Montenay-Garestier, T.; Hélène, C. *J. Phys. Chem.* **1990**, *94*, 968−977.
(78) Marty, A.; Bourdeaux, M.; Dell'Amico, M.; Viallet, P. *Eur. Biophys. J.* **1986**, *13*, 251−257.
(79) Brauns, E. B.; Madaras, M. L.; Coleman, R. S.; Murphy, C. J.; Berg, M. A. *J. Am. Chem. Soc.* **1999**, *121*, 11644−11649.
(80) Kelley, S. O.; Barton, J. K. *Chem. Biol.* **1998**, *5*, 413−425.
(81) Nastasi, M.; Morris, J. M.; Rayner, D. M.; Seligy, V. L.; Szabo, A. G.; Williams, D. F.; Williams, R. E.; Yip, R. W. *J. Am. Chem. Soc.* **1976**, *98*, 3979−3986.

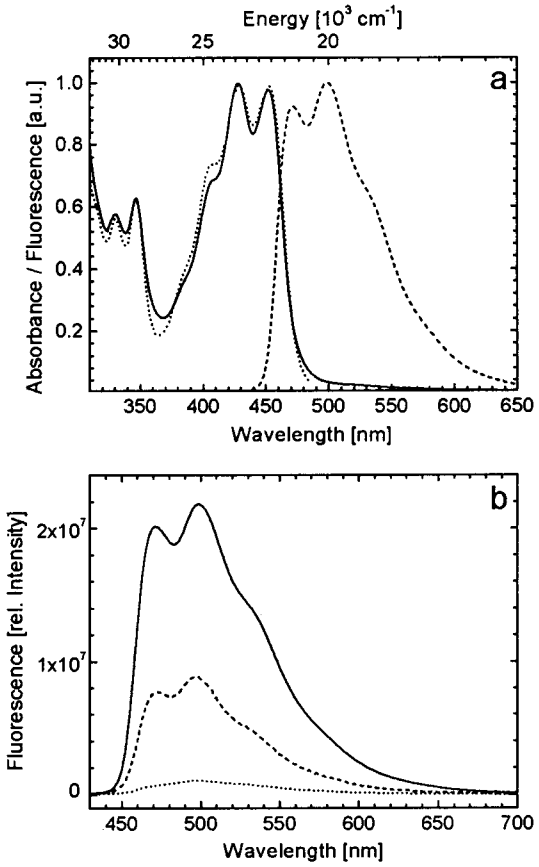

Figure 1. (a) Normalized absorption (—), fluorescence emission (- - -), and fluorescence excitation (•••, emission at 500 nm) spectra of X^+ in duplex X^+(AT) at 283 K. (b) Comparison of the relative fluorescence intensity measured in duplexes X^+(AT) (—), 3′-X^+AG (- - -), and 3′-X^+G (•••).

infra) was detected compared to that in analogue duplexes with guanine. Independent of direction along the helix (3′ or 5′), almost complete quenching of X^+ fluorescence was found for duplexes X^+Z, X^+G, and X^+AZ, whereas X^+AAZ, X^+AG, and X^+AAG showed significant fluorescence yields.

In all duplexes, the fluorescence excitation spectra, at both 470 and 500 nm emission wavelengths, closely follow the X^+ absorption spectrum as shown for X^+(AT) in Figure 1a.

Although not shown, the CD spectra of all X^+-labeled duplexes investigated display a positive band at ~280 nm and a negative band at 250 nm, indicative of an overall B-form DNA structure.[82,83] In the visible and near UV, all duplexes have a strong, negative CD band (which is a mirror image to the X^+ $S_0 \rightarrow S_1$ absorption band) and a positive CD band at 350 nm where the $S_0 \rightarrow S_2$ band of X^+ absorbs. These features are indicative of a well-defined, rigid X^+ environment in these duplexes.

2.2. Femtosecond Transient Absorption Spectroscopy. Femtosecond pump−probe measurements were performed using two amplified Ti:sapphire laser systems differing in time resolution and excitation wavelength. For measurements with a probe wavelength of 450 nm excitation pulses at 390 nm were used, while for all other measurements the excitation was tuned to 455 nm (for details see Experimental Section). Both 390 and 455 nm pump pulses allow for excitation of the $S_0 \rightarrow S_1$ transition of the chromophore (Figure 1a). Unless explicitly stated otherwise the experiments presented in this section refer to duplexes labeled by 3′-X^+ in Chart 1. All kinetic data of section 2.2 are compiled in Table 1.

Table 1. Forward and Backward Charge-Shift Rates k_1 and k_2

duplex	k_1, s^{-1} [a]	k_2, s^{-1} [b]
3′-X^+G	2.6×10^{11}	2.9×10^{10}
5′-X^+G	1.7×10^{11}	2.0×10^{10}
3′-X^+AG	8.9×10^{7}	−
5′-X^+AG	2.8×10^{7}	−
3′-X^+Z	1.4×10^{12}	1.6×10^{11}
5′-X^+Z	1.1×10^{12}	1.3×10^{11}
3′-X^+AZ	9.1×10^{10}	1.0×10^{10}
5′-X^+AZ	8.3×10^{10}	5.9×10^{9}
3′-X^+AAZ	7.4×10^{7}	−
5′-X^+AAZ	3.0×10^{7}	−

[a] Forward hole-shift rates calculated from excited-state lifetimes according to $k_1 = \tau_{obs}^{-1} - \tau_0^{-1}$, where τ_0 is the excited-state lifetime of the reference duplex X^+(AT), 18 ns and τ_{obs} is the excited-state lifetime of a sample with hole transfer. [b] Rates for the backward charge shift obtained from radical lifetimes and the ground-state recovery times.

Excited-State Dynamics of the Reference Duplex X^+(AT). Upon photoexcitation of X^+ in this duplex, several transient features are observed in the spectral region between 450 and 850 nm. The different spectral regions correspond to excited-state absorption (550−850 nm), ground-state recovery (450 nm), and stimulated emission (470−530 nm). Figure 2a shows the kinetic traces of X^+(AT) obtained at probe wavelengths of 650, 500, and 450 nm. All traces are monoexponential[84] and show lifetimes >5 ns. In a previous communication,[85] the kinetics at these wavelengths were investigated using nanosecond time-resolved absorption spectroscopy on a laser system allowing probing in the nanosecond-to-millisecond time window. The monoexponential lifetime of $^1(X^+)^*$, measured using 455 nm pump/650 nm probe pulses, is 18 ns. This value is in reasonable agreement with the fluorescence decay time of 22.8 ns for a similar X^+-labeled, all-(A:T) duplex reported by Tanaka and co-workers.[32]

Hole-Transfer Dynamics in the Different G- and Z-Containing Duplexes. When a G:C base pair is placed next to X^+, duplex 3′-X^+G, a new positive feature is observed in the stimulated emission region (Figure 2b) which rises with a time constant of 3.8 ps and decays in 35 ps. Previous transient absorption spectroscopy measurements on a similar acridine derivative have shown that these chromophores have a broad radical ($X^•$) absorption band with a maximum around 500 nm.[86,87] Because the decay time of this positive band matches the observed recovery time of the X^+ ground state (450 nm probe) and the time scale for the decay of the red positive transient (650 nm probe data shown in Figure 2b), we assign this new band to absorption of the product state $X^•$ formed via a photoinduced hole-transfer reaction from $^1(X^+)^*$ to G. We note that we find no evidence for absorption of the guanine radical cation at 450 nm,[88] a result not unsurprising since the

(82) Jin, R.; Gaffney, B. L.; Wang, C.; Jones, R. A.; Breslauer, K. J. *Proc. Natl. Acad. Sci. U.S.A.* **1992**, *89*, 8832−8836.

(83) Lu, M.; Guo, Q.; Kallenbach, N. R. *Biochemistry* **1993**, *32*, 598−601.

(84) The fast recovery features seen in the kinetics under 390 nm pump/450 nm probe conditions were instrument limited. They seem to be an artifact as supported by the identity of excited-state decay traces probed in either the $S_1 \rightarrow S_n$ absorption (650 nm) or by stimulated emission (500 nm).

(85) Davis, W. B.; Naydenova, I.; Haselsberger, R.; Ogrodnik, A.; Giese, B.; Michel-Beyerle, M. E. *Angew. Chem.* **2000**, *112*, 3795−3798.

(86) Neta, P. *J. Phys. Chem.* **1979**, *83*, 3096−3101.

(87) Jones, G., II; Farahat, M. S.; Greenfield, S.; Gosztola, D. J.; Wasielewski, M. R. *Chem. Phys. Lett.* **1994**, *229*, 40−46.

(88) Candeias, L. P.; Steenken, S. *J. Am. Chem. Soc.* **1989**, *111*, 1094−1099.

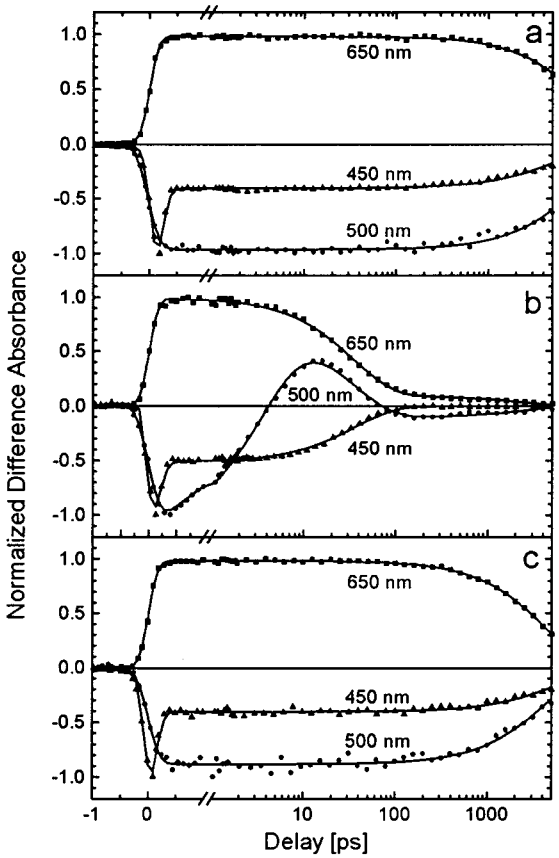

Figure 2. Transient pump−probe kinetics measured in duplexes (a) X^+(AT), (b) 3′-X^+G, and (c) 3′-X^+AG [390 nm, ∼150 fs pump pulses were used for excitation when probing at 450 nm, and 450 nm, ∼200 fs pump pulses were used when probing at all other wavelengths (500−850 nm)]. The probe wavelength used for each kinetic trace is noted in (a−c). The time scale is linear from −1 to 1 ps and logarithmic from there on. The solid lines are nonlinear least-squares fits to the data, whose fit parameters are listed in the Supporting Information.

extinction coefficient of $G^{\bullet+}$ at this wavelength is only ∼2000 M^{-1} cm^{-1} as compared to $\epsilon \approx 9500$ M^{-1} cm^{-1} for the 9-amino-6-chloro-2-methoxyacridine chromophore.[89,90]

In X^+(AT) the positive feature at 650 nm is excited singlet state absorption. However, in the duplex 3′-X^+G both $^1(X^+)$* and X• absorb at this wavelength, and as hole transfer occurs there is an evolution between the two states which masks the rise characteristics of X•. For probe wavelengths tuned further to the red (>700 nm) the absorption from the excited state dominates yielding kinetics with two decay components: a 4 ps component corresponding to the excited-state lifetime and a 35 ps component corresponding to the lifetime of the radical. An important feature of all measurements is that both the charge-shift rate and the back-transfer rate are monoexponential and there is only a small fraction (<10%) of long-lived background signal observed in our transient kinetics.

Placement of one A:T pair between X^+ and guanine (3′-X^+-AG) changes the observed transient absorption features back to those found for the reference system X^+(AT), Figure 2c. The X• band is not observed, and the kinetics of the ground-state recovery of X^+, as well as the decay of $^1(X^+)$* monitored using the stimulated emission lifetime and the lifetime of the 540−850 nm band, are again monoexponential with lifetimes >5 ns.

(89) Wilson, W. D.; Lopp, I. G. *Biopolymers* **1979**, *18*, 3025−3041.
(90) Asseline, U.; Delarue, M.; Lancelot, G.; Toulmé, F.; Thuong, N. T.; Montenay-Garestier, T.; Hélène, C. *Proc. Natl. Acad. Sci. U.S.A.* **1984**, *81*, 3297−3301.

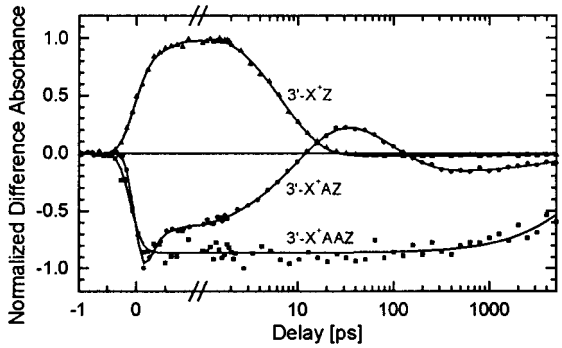

Figure 3. Transient pump−probe kinetics measured in duplexes 3′-X^+Z (▲), 3′-X^+AZ (●), and 3′-X^+AAZ (■), using 450 nm, ∼200 fs pump pulses and either 500 or 530 nm probe pulses. The time scale is linear from −1 to 1 ps and logarithmic from there on. The solid lines are nonlinear least-squares fits to the kinetic data, whose parameters are listed in the Supporting Information.

Nanosecond-transient absorption measurements yielded the kinetics listed in Table 1 for this duplex.[85] Both the ground-state recovery and the excited-state decay are faster in 3′-X^+AG than those measured in X^+(AT), implying a guanine-specific quenching mechanism for $^1(X^+)$* in this duplex. When two A:T base pairs are placed between X^+ and G, duplex 3′-X^+AAG, there is no excited-state quenching of X^+, indicating an absence of hole transfer in this duplex.

When the Z:C base pair is placed next to X^+, duplex 3′-X^+Z, the transient absorption features resemble those observed for 3′-X^+G. The product state X•, monitored at 500 nm, is formed within 700 fs and decays with a lifetime of 6.4 ps (Figure 3). The ultrafast decay of $^1(X^+)$* is consistent with the observation that 3′-X^+Z is almost nonfluorescent in steady-state measurements (section 2.1.). Once again, single-exponential forward charge-shift and back-transfer kinetics are observed in this duplex, with negligible background signal.

Unlike in duplex 3′-X^+AG, the placement of a single A:T pair between X^+ and Z in duplex 3′-X^+AZ does not result in the disappearance of the X• signal, Figure 3. Both the forward charge-shift and the back-transfer lifetime slow by a factor of ∼15 with respect to their counterparts in 3′-X^+Z (Table 1). However, placing two A:T base pairs between X^+ and Z does result in transient dynamics resembling those of duplex 3′-X^+AG, (Figures 2c and 3). In 3′-X^+AAZ there is no observation of X•, and the kinetics of ground-state recovery and excited-state decay are >5 ns. Nanosecond transient absorption spectroscopy shows that the kinetics of ground-state recovery and excited-state decay of X^+ are monoexponential with identical rates, and faster than those observed in X^+(AT).

Directionality of the Hole-Transfer Dynamics. In addition to the 3′-X^+ duplexes we also studied hole transfer occurring in the opposite helical direction (5′-X^+ duplexes). In all 5′-X^+ duplexes spectral features identical to those discussed above for their corresponding 3′-X^+ counterparts are observed. The lifetimes of the excited state and the X• state measured for duplexes with the same distance between the X^+ hole donor and an acceptor nucleobase are of the same order magnitude, with rates in the 3′-X^+ duplexes consistently larger than those in the 5′-X^+ duplexes (Table 1).

3. Discussion

Preliminary Remarks. The steady-state absorption and fluorescence spectra in all of these X^+-labeled duplexes are characteristic of an X^+ chromophore covalently bound in an abasic site.[74] The melting points of X^+ duplex modifications[75]

were higher than those of abasic DNA and native DNA. Thus, it is clearly demonstrated that hybridization and incorporation of X^+ into an abasic site are cooperative and that the π-stacked acridine ring compensates the destabilization due to the missing thymine. CD spectra confirm that the overall structure of the duplexes is largely B-form and that the environment around the X^+ chromophore is highly ordered. Details on the structure and the chromophore's binding geometry are expected from differential NMR studies which are in progress.[91]

Since similar kinetics and transient absorption spectra are observed for hole transfer between X^+ and a hole acceptor at a fixed base pair separation in either helical direction of the duplex (Table 1), the following discussion is restricted to the phenomenology of 3′ duplexes. We note, however, that by a factor of 2, the electron-transfer rates tend to be larger in 3′ duplexes than those in 5′ duplexes. This effect mirrors the asymmetry of the electronic interaction between the nucleobases in the two helical directions.[36] Henceforth, we will drop the 3′-label on the duplexes and refer to them only by the local sequence surrounding the X^+ chromophore. The kinetics and transient absorption dynamics in these duplexes are calibrated with respect to the kinetic features of the reference system X^+(AT), which clearly show that within the excited-state lifetime A:T pairs are not oxidized.

The femtosecond time-resolved absorption experiments presented in the preceding section provide detailed information on the phenomenology of hole-injection dynamics in X^+-modified DNA duplexes. The excitation and probing conditions given for these duplexes allow independent access to the kinetics of $^1(X^+)^*$ decay and X^+ ground-state recovery, as well as to the formation and decay rates of the charge-transfer product state $X^\bullet$. Before entering a more detailed discussion of these experiments, we would like to state that the crucial information on the nature of the steep distance dependence of hole-injection rates for X^+-modified duplexes can be directly extracted from the data set in the Experimental Results without any assumptions or kinetic modeling. The kinetic features of the X^+/DNA duplexes clearly point to the interplay of two effects: the decrease of the electronic couplings and a concomitant increase of the activation energy for hole transfer with increasing distance between X^+ and the electron donor species, G or Z.

The following discussion of mechanism and distance dependence of the hole-transfer rates has to be kept on a qualitative level since thus far the data sets are too incomplete for applying the full machinery of electron-transfer theory. Nevertheless, whenever we try to rationalize the kinetics in the framework of electron-transfer theory, this attempt has to be based on independent estimates of the low-frequency reorganization energy λ_s. Reorganization energies in DNA may be rather complex, reflecting the response of the nucleobases, of the backbone, and of the aqueous solvent on the change in charge distribution associated with the electron-transfer process. The most recent experimental value of λ_s arises from the work of Lewis et al.,[92] where data analysis in the framework of a semiclassical approach yields $\lambda_s = 0.2-0.4$ eV for stilbene-capped DNA hairpins. Similar values have been proposed earlier.[28] λ_s-values in this range follow also from the recent analysis of reaction yields associated with hole hopping after thermal injection in the Giese-type DNA systems.[33,34]

Hole Transfer in X^+G and X^+Z. The forward hole-transfer rates k_1 in the duplexes X^+G and X^+Z, where the hole donor and acceptor are in direct contact, are 2.6×10^{11} s^{-1} and 1.4×10^{12} s^{-1}, respectively, and as mentioned before, essentially single-exponential. Small, long-lived background signals are attributed to a minority (<10%) of modified duplexes displaying an extrahelical X^+ geometry. This feature of monoexponential electron-transfer kinetics pertains to all duplexes studied in this paper. The ultrafast rate measured for X^+Z implies that hole transfer occurs under either activationless ($\Delta G \approx \lambda$), or slightly inverted conditions ($\Delta G > \lambda$). The above estimate of λ limits the driving force $-\Delta G$ to the range 0.2−0.4 eV. Assuming the oxidation potential of G to be by ~0.1−0.3 eV higher than that of Z.[22,80] It follows that $-\Delta G \approx 0.0-0.3$ eV in X^+G. The respective back-transfer rates, k_2, are for both systems slower than the forward rates, k_1, by a factor of 9. In contrast to k_1 the back transfer rate is characterized by a large driving force (<−2.3 eV) resulting from 2.7 eV excited-state energy of $^1(X^+)^*$ and the limits of ΔG for k_1. Such relatively "small" values for k_1/k_2 can be explained when the explicit formalism underlying eq 1 is applied.[50]

How do the kinetic rates of X^+-modified DNA relate to other DNA charge-transfer duplexes reported in the literature? In femtosecond absorption spectroscopy Lewis et al. have investigated synthetic DNA hairpins containing the neutral stilbene-4-4′-dicarboxamide as a photoexcited hole donor.[55,92] In contrast to the charge-shift reactions of the protonated acridine intercalator X^+ the stilbene derivative undergoes charge separation and recombination. Despite all of the differences between X^+ and the stilbene derivative, the kinetic pattern in the nearest-neighbor hairpin ($k_1 = 1.0 \times 10^{12}$ s^{-1} and $k_2 = 4.3 \times 10^{10}$ s^{-1})[55] and in the X^+G duplex ($k_1 = 2.6 \times 10^{11}$ s^{-1} and $k_2 = 2.9 \times 10^{10}$ s^{-1}) can be qualitatively compared. The different ratios of the forward-to-back transfer rates, $k_1/k_2 \approx 23$ for the stilbene system and $k_1/k_2 \approx 9$ for X^+G are to be attributed to the deeper inversion of k_2 in the case of the stilbene DNA hairpin. The replacement of G by Z in both systems results in an acceleration of the hole-transfer rates by a factor of 5. Thus, at least in the case of nearest neighbor charge transfer in duplex DNA, charge-shift and charge-separation reactions tend to show similar kinetic behavior.

Hole Transfer in X^+AG and X^+AAG. From the data in Table 1, it follows that the ratio of the forward rates $k_1(X^+G)/k_1(X^+AG)$ is 2900. In case we would ignore the mechanistic definition of β according to eq 1 and extract its value from these two data points where one of them applies to direct contact and the other one to superexchange-mediated transfer, an unphysically large β value of 2.3 Å^{-1} would result. This value is even higher than the 1.5 Å^{-1} attenuation factor reported by Fukui et al.[32] and in even more dramatic contrast to the previously reported β values of 0.6−0.8 Å^{-1}.[27,29,44,55] Such a steep distance dependence is also supported by the observation of no fluorescence quenching in X^+AAG, indicating that the hole-transfer rate in this duplex must be much slower than the 18 ns excited-state lifetime of X^+ in X^+(AT). Already at this stage of the discussion a β value of the order of 2.0 Å^{-1} points to the fact that in X^+-labeled DNA duplexes the electronic coupling V cannot be the sole factor determining the distance dependence of the injection rate. The large β value is rather the fingerprint of two superimposed effects: a decrease of the superexchange-mediated electronic couplings V which is accompanied by a growing-in of the activation energy with increasing X^+−G distance. This explanation is consistent with the finding that in the system X^+AG the product state $X^\bullet$ is not observed, which is indicative of a fast (less activated) back-transfer rate k_2 as compared to the forward rate k_1. In summary,

(91) In cooperation with C. Griesinger, (University of Frankfurt).

(92) Lewis, F. D.; Kalgutkar, R. S.; Wu, Y.; Liu, X.; Liu, J.; Hayes, R. T.; Miller, S. E.; Wasielewski, M. R. *J. Am. Chem. Soc.* **2000**, *122*, 12346−12351.

in the X^+/DNA system there are two hole-transfer regimes which differ with respect to the activation energy of the forward rate k_1: for the direct contact system X^+G, and also for X^+Z and X^+AZ (see below) k_1 exceeds k_2, while the opposite is true for the duplexes X^+AG and X^+AAZ.

To put the concept of a distance-dependent activation energy in X^+-labeled duplexes to test, the injection reaction in the system X^+AZ should be faster than in X^+AG since replacing G by Z is expected to increase the driving force ΔG. This expectation is also consistent with the nearest-neighbor behavior as discussed before.

Hole Transfer in X^+AZ and X^+AAZ. In contrast to the large ratio, $k_1(X^+G)/k_1(X^+AG) = 2900$, the replacement of G by Z leads to $k_1(X^+Z)/k_1(X^+AZ) = 15$. This ratio coupled with the observation of the $X^{\bullet}AZ^{\bullet+}$ intermediate state indeed points to a smaller activation energy as compared to that of the system X^+AG. A reduction factor of 15 per A:T base pair between a hole donor and acceptor in DNA would correspond to $\beta \cong 0.8$ $Å^{-1}$, a value similar to that observed in the previous transient absorption experiments of Lewis et al.[55] and in the Giese-type[44] yield studies. In contrast to X^+AG, in X^+AZ the back-transfer rate k_2 is observed, whereas the dynamics in duplex X^+AAZ are similar to those of X^+AG where k_2 is not observed. This phenomenology is to be expected for a change in charge-transfer mechanism from (nearly) activationless hole transfer in X^+AZ to thermally activated injection kinetics in X^+AAZ. Hence, these experiments involving nucleobase G/Z replacement independently justify the assignment of the large β value to a change of mechanism involving the energy parameters.

In the duplex X^+AZ the ratio of rates $k_1/k_2 = 10 \pm 2$. As in the direct contact systems, X^+G and X^+Z, this ratio is expected to predominantly reflect forward hole transfer in the activationless or slightly activated regime of the Marcus expression while the back-transfer dynamics occur under inverted conditions. Since in contrast to the nearest-neighbor systems the hole-transfer dynamics in this duplex are mediated by superexchange interaction due to the intervening A:T base pair, this ratio may also include a smaller superexchange coupling for k_2 as compared to k_1 caused by an increased vertical energy difference between the state $X^{\bullet}AZ^{\bullet+}$ and the A:T bridge.

Distance-Dependent Activation Energy in X^+-Labeled DNA Systems. Concerning the mechanism by which distance-dependent activation energies arise, two intrinsically different scenarios have to be envisaged: (i) the predominant distance-dependent effect is a loss of driving force due to excited-state relaxation of $^1(X^+)^*$ competing with charge transfer, and (ii) the reorganization energy λ_s in this charge-shift reaction displays a distance dependence on purely electrostatic grounds.[52,53] Falling back on the excited-state relaxation phenomena of X^+ as published by Hélène and co-workers,[77] it seems reasonable to base the following discussion of the kinetic consequences of a distance-dependent thermal activation on such relaxation effects in X^+/DNA oligomers.

In the absence of excited-state relaxation in the system X^+AG the forward rate k_1 is expected in the time window 50−100 ps when $\beta \approx 0.8$ $Å^{-1}$ is implied. In reality k_1 appears to be in the nanosecond range. If we allow for X^+* relaxation to occur in this time window, the nanosecond rates for X^+AG reflect the superposition of two effects: (i) a decrease of the superexchange electronic coupling with increasing X^+−G distance which slows down k_1 and thus allows (ii) an X^+*-specific relaxation process to compete with charge injection after a specific donor−acceptor separation is reached. At larger X^+−G separation the relaxation rate is assumed to be faster than the charge-transfer rate out of the initial Franck−Condon state. Since the relaxation process is expected to affect the driving force ΔG of the charge injection, the latter one becomes thermally activated. If relaxation would influence predominantly the electronic couplings V, the ratio k_1/k_2 would remain fairly constant, and X should be observed in the transient absorption of X^+AG in contrast to reality.

Scheme 1. Kinetic Scheme for the Distance-Dependent Change of Mechanism in Case Excited-State Relaxation Being the Origin of the Increase of Activation Energy at Larger Distances[a]

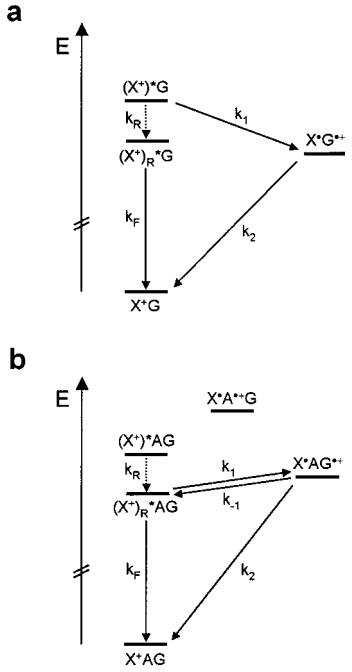

[a] Scheme 1a representing X^+G is also a prototype for X^+Z and X^+AZ, whereas Scheme 1b is valid for the dynamics in X^+AG and X^+AAZ. In Scheme 1b, $X^{\bullet}A^{\bullet+}G$ acts only as a superexchange mediator and is not an observable intermediate.

In Scheme 1 the dynamics of activationless or slightly activated (1a) and thermally activated electron transfer after X^+ excited-state relaxation (1b) are illustrated. If the steady-state approximation holds, the measured decay rate of $^1(X^+)^*$ in Scheme 1b is given by

$$k_{obs} = k_F + \frac{k_2 k_1}{k_2 + k_{-1}} \tag{3}$$

where k_F is the rate of fluorescence from the relaxed excited state $^1(X^+)_R^*$. The validity of the steady-state approximation is strongly supported by the monoexponentiality and identical time constants of the X^+ excited-state decay and ground-state recovery in these duplexes.[85] Equation 3 can be rearranged to

$$k_1 = \frac{k_{obs} - k_F}{1 - \frac{(k_{obs} - k_F)}{k_2}\exp(\Delta G/k_B T)} \tag{4}$$

where ΔG is the energetic difference between the states $^1(X^+)_R^*$ and $X^{\bullet}$. Monoexponential kinetics in these duplexes can only be observed if $k_1 \ll k_2$. For the purposes of the following discussion, we assume an arbitrary upper limit of $k_2 > 5k_1$. Therefore, once an appropriate expectation value of k_2 is set, one may obtain an estimate for the maximum values of both ΔG and k_1. For instance, if we assume that X^+ excited-state

relaxation primarily affects k_1 and not k_2 (due to k_2 lying in the Marcus inverted region) and take a reasonable value of 15 for the decrease in electronic coupling upon insertion of one A:T base pair, then $k_2 \approx 1.9 \times 10^9$ s^{-1} in X^+AG and $k_2 \approx 6.7 \times 10^8$ s^{-1} in X^+AAZ. These values of k_2 lead to the limits of $k_1 < 3.8 \times 10^8$ s^{-1} in duplex X^+AG and $k_1 < 1.3 \times 10^8$ s^{-1} in X^+AAZ. From these estimates we assert that after X^+ relaxation we are in the steady-state limit where $k_{obs} - k_F = k_1$. Since $k_{obs} - k_F$ is 8.9×10^7 s^{-1} in X^+AG and 7.4×10^7 s^{-1} in X^+AAZ, ΔG_{max} in the Z duplex is +0.033 eV and +0.068 eV in the G duplex. We note that while the difference in the upper limits of $\Delta G = 0.035$ eV for the two duplexes is by a factor of 2−3 smaller than the lower limit 0.1 eV of the oxidation potential difference between Z and G, the relative values are consistent with Z being the easier of the two nucleobases to oxidize in duplex DNA. On the other hand, the tacit assumptions of invariant electronic couplings and reorganization energies in G- and Z-containing sequences and identical relaxation patterns might not be valid.

Although a time- and distance-dependent energy loss due to relaxation explains the large β value, the task for the future is a quantitative modeling not only of the scenario of X^+ excited-state relaxation but also of the influence of a distance-dependent reorganization energy on the electron-transfer rates. With respect to the time scale and the contribution of excited-state relaxation to the activation energy, the necessary information will be provided by measurements of the dynamic Stokes shift. In addition, temperature-dependent studies may lead to independent information on the relevant energetic parameters in these duplexes. To estimate the contribution of distance-dependent reorganization energies to the activation term, efforts are directed toward a NMR structure of the X^+/DNA system, quantum chemical computations, and a detailed assessment of the nature of the heterogeneous dielectric environment of the DNA core.[93]

Comparison to Previous Hole-Transfer Experiments in X^+-Labeled DNA Duplexes. The duplexes 3′-X^+G, 5′-X^+G, 3′-X^+AG, and 5′-X^+AG are direct analogues of the DNA duplexes studied earlier by Fukui and Tanaka.[32,74] In these studies, fluorescence quantum yields and fluorescence decay times were used to investigate the distance dependence of electron transfer in DNA between 9-alkylamino-6-chloro-2-methoxyacridine (covalently attached to the DNA through a slightly different linker from that in X^+) and a guanine nucleobase. Most likely due to instrument limitation the forward charge-shift rates in the X^+G duplexes have not been resolved. On the other hand, the slow hole-injection rates derived from time-resolved fluorescence measurements on 3′-X^+AG duplexes in the previous work[32,74] were confirmed in this laboratory and are in very good agreement with the pump−probe measurements in this paper. A detailed study of fluorescence dynamics in different duplexes with emphasis on time-dependent Stokes shift are in progress. In addition, the dependence of k_1 on the helical direction of transfer, for example comparison of 3′-X^+AG and 5′-X^+AG, is also reproduced faithfully by the transient absorption data. The ratio $k_1(X^+G)/k_1(X^+AG)$ from these measurements is 2900, which predicts an apparent value of β in DNA of 2.3 Å^{-1}, a value even higher than the value given by Fukui and Tanaka, $\beta = 1.5$ Å^{-1}. As discussed in the section above, this large attenuation factor is due to a superposition of the decrease of coupling and an increase of the activation energy, a result inaccessible in fluorescence measurements alone.

(93) In cooperation with M. D. Newton, N. Rösch, and A. A. Voityuk.

4. Conclusions

Using transient absorption spectroscopy, we have studied the distance dependence of charge-shift dynamics between the covalently attached, photoexcited electron acceptor 9-alkylamino-6-chloro-2-methoxyacridine (X^+), selectively intercalated into a DNA duplex at an artificial abasic site, and either a guanine (G) or 7-deazaguanine (Z) base as an electron donor, with the number of A:T base pairs between the donor and acceptor as the only variable parameter. Monoexponential electron-transfer rates point to well-defined electronic couplings in these duplexes. Since these couplings reflect short-range interactions, one majority incorporation site for the X^+ chromophore is highly probable. The absence of distributed kinetics even on the subpicosecond time scale shows that structural fluctuations[94] on any longer time scale are not reflected by a distribution of electronic couplings between X^+ and the nucleobases within the base stack. This invariance could be the result of strong $\pi-\pi$ and dipolar interactions between the intercalated chromophore and the neighboring nucleobases, interactions which lead to an increased rigidity of the local structure around the intercalator and the X^+-specific features observed in the visible and near-UV CD spectrum of these duplexes.

This work was motivated by the optimal conditions for long-range hopping studies provided by this system: (1) injection occurs via a charge-shift reaction with a minimized Coulombic well and (2) on the basis of energetics and the slow forward charge-shift rate measured by Tanaka and Fukui in duplex 3′-X^+AG, we expected charge hopping in a sequence such as 3′-X^+AGAG to favorably compete with the back charge transfer. The escape probability of the hole from the initially oxidized guanine was further expected to be enhanced by the small electronic couplings between X^+ and the proximate G, as indicated by the large $\beta = 1.5$ Å^{-1} reported in Tanaka's previous work.[32]

In the context of utilizing the system for a study of hole-hopping dynamics in duplex DNA, the injection kinetics were revisited using femtosecond-resolved transient absorption spectroscopy. The key results of this study are summarized as follows:

In X^+/DNA oligomers the distance dependence has been shown to be complex, involving contributions of both electronic couplings and energy parameters. Tentatively, the experimental data have been self-consistently interpreted within the frame of a relaxation model where forward charge-shift dynamics have to compete with an excited-state relaxation in the singlet manifold of photoexcited X^+. This relaxation has to proceed with a rate of approximately 2×10^{10} s^{-1}, and after relaxation we observe features typical for activated charge transfer. In this scenario where the forward transfer is the rate-determining step, no charge transfer intermediate states are observed, and the charge recombination dynamics are not resolved. On the other hand, samples with hole-injection rates significantly faster than the relaxation display regular behavior with forward rates being a factor of approximately 10 faster than the back-transfer rates. The combination of a decrease in couplings with increasing donor−acceptor distance and a concomitant increase of activation energy leads to an apparent attenuation value β of around 2 Å^{-1}.

Activated electron transfer in X^+-labeled DNA may be utilized to map out in situ the relative energetics of purine bases in the duplex. Along these lines, the relative ease of oxidation

(94) Cheatham, T. E., III; Kollman, P. A. *Annu. Rev. Phys. Chem.* **2000**, *51*, 435−471.

of single guanines and GG and GGG tracts has already been reported.[85]

From the relative hole-transfer rates in the systems X^+Z and X^+AZ a "two-point" attenuation factor of 0.8 $Å^{-1}$ is obtained. This value is in perfect agreement with the first points on a ln *k* vs *R* plot in the stilbene/DNA system. In the more general context of relating fluorescence data to charge-transfer dynamics, the discrepancy in the conclusions of the previous work and those of this paper is indicative of the inherent danger of reliance on an experimental method which cannot follow the formation and decay of an intermediate charge-separated product state, for example, $X^{\bullet}G^{\bullet+}$.

However, at the present stage, this excited-state relaxation scenario provides only an ad hoc explanation of the experimental findings. In a future, more detailed treatment of the observed steep distance dependence of the injection rates in the X^+/DNA system the loss of driving force via relaxation has to be quantified and related to the influence of distance-dependent reorganization energies on the attenuation factor β.

5. Experimental Section

Oligonucleotides. All DNA strands used in this study were ordered from Eurogentec Köln (Germany), delivered lysophilized after polyacrylamide gel electrophoresis (PAGE) purification, and stored at −10 °C under the exclusion of light until shortly before use. Stock solutions of complementary single strands were made by dissolving each strand in a 10 mM Na_2HPO_4/NaH_2PO_4, 100 mM NaCl, pH 7.2 buffer solution. These stock solutions were mixed in a 1 × 10 mm quartz cuvette with a 10% excess of non-X^+-modified counter strand present to help ensure that all X^+ chromophores would be located in a DNA duplex. Hybridization was performed by heating the mixed single strands to 80 °C, followed by slow cooling to room temperature over 2 h. All samples had an adenine base opposite to X^+ on the counter strand. The hybridized spectroscopic samples were stored at 4 °C prior to their characterization.

Steady-State Spectra. Steady-state absorption spectra were obtained using a UV−vis spectrometer (Perkin-Elmer Lambda 2S) with 2.0 nm resolution. For measurement of steady-state fluorescence spectra and fluorescence excitation spectra a spectrofluorometer (Spex Fluorolog-2 model F212I) with 1.7 nm resolution or better was used. All UV−vis and fluorescence spectra were taken at 283 K. Circular dichroism spectra were obtained on a Janus Scientific Jasco-715 CD spectrometer using X^+-DNA samples made by diluting ∼5 μL of each spectroscopic sample in a 4 × 10 mm quartz cuvette with additional buffer until an optical density of 1.0 at 260 nm was obtained.

Transient Absorption Spectroscopy. Femtosecond time-resolved transient absorption measurements were performed using two separate laser systems. For measurements with a pump wavelength at 455 nm a commercial Ti:sapphire oscillator/regenerative amplifier system (Coherent/BMI) with a time resolution better than 200 fs and a repetition rate of 1 kHz was used. This laser system has been previously described in detail.[95,96] Briefly, to generate pulses at 455 nm, the output at 780 nm was frequency-doubled and used to pump an optical parametric generator, followed by a two-step optical parametric amplifier (OPG/OPA, BMI Venturi II). With this apparatus, we were able to produce 150 fs pulses at 455 nm with 1 μJ energy. Probe pulses were generated by selecting a 15 nm wide portion out of a white light continuum generated by focusing 1−2 μJ pulses at 780 nm in a 2 mm sapphire crystal.

In the second system, ∼150 fs, 390 nm pump pulses with an energy of ∼100 μJ/pulse were obtained by frequency doubling the 1 kHz, 780 nm output of a home-built amplified Ti:sapphire laser in a 2 mm BBO crystal. The design of the laser system is similar to the one described by Hochstrasser and co-workers.[97] Probe pulses between 450 and 700 nm were produced by focusing a small fraction of the amplifier output at 780 nm into a 2 mm sapphire crystal. In both systems, pump and probe pulses were focused on the sample under a small angle. The relative polarizations were set to magic angle (54.7°) to avoid rotational depolarization effects.

Samples had optical densities of about 0.3 at 450 nm in a 1-mm-path-length quartz cuvette (concentration ∼0.3 mM). The cuvette was moved perpendicularly to the probe beam to avoid sample bleaching. Steady-state absorption spectra were taken before and after time-resolved measurements to check for sample degradation. The temperature of the samples was held fixed to 10 ± 2 °C during all measurements using a home-built temperature controller. Deoxygenation of the samples by purging with argon had no effect on the measured kinetics.

Nanosecond decay times were determined using an absorption laser system that has been described in detail previously.[98] Briefly, 450 nm pump pulses were generated by pumping a coumarin 120 dye laser with the third harmonic of a Nd:YAG laser. Probe pulses at either 420 or 590 nm were generated by a N_2-laser pumped-dye laser. The delay time between excitation and probing pulse was adjusted electronically. The time resolution of this setup was ∼2 ns.

Acknowledgment. We thank Dr. Izabela Naydenova and Reinhard Haselsberger for performing the nanosecond transient absorption measurements reported here. In addition, we are very grateful for detailed discussions with Professor M. Bixon and Professor J. Jortner. This work was supported by the Fonds der Chemischen Industrie and the Bundesministerium für Bildung und Forschung (S.H.) and the Alexander von Humboldt Stiftung (W.B.D.). Financial support from the Deutsche Forschungsgemeinschaft (SFB 377) and Volkswagenstiftung is, in addition, gratefully acknowledged.

Supporting Information Available: Tables showing the numerical parameters of the fit functions displayed as solid lines in Figures 2 and 3, and time-resolved transient absorption spectra of duplex 3′-X^+G (PDF). This material is available free of charge via the Internet at http://pubs.acs.org.

JA010976R

(95) Pöllinger, F.; Musewald, C.; Heitele, H.; Michel-Beyerle, M. E.; Anders, C.; Futscher, M.; Voit, G.; Staab, H. A. *Ber. Bunsen-Ges. Phys. Chem.* **1996**, *100*, 2076−2080.

(96) Lossau, H.; Kummer, A.; Heinecke, R.; Pöllinger-Dammer, F.; Kompa, C.; Bieser, G.; Jonsson, T.; Silva, C. M.; Yang, M. M.; Youvan, D. C.; Michel-Beyerle, M. E. *Chem. Phys.* **1996**, *213*, 1−16.

(97) Wynne, K.; Reid, G. D.; Hochstrasser, R. M. *Opt. Lett.* **1994**, *19*, 895−897.

(98) Volk, M.; Aumeier, G.; Langenbacher, T.; Feick, R.; Ogrodnik, A.; Michel-Beyerle, M. E. *J. Phys. Chem. B* **1998**, *102*, 735−751.